Soft Robotics

Journal Name: http://mc.manuscriptcentral.com/master0

Paper-based Robotics with Stackable Pneumatic Actuators

Journal:	*Soft Robotics*
Manuscript ID	SORO-2020-0023
Manuscript Type:	Original Article
Date Submitted by the Author:	12-Feb-2020
Complete List of Authors:	Zou, Xiyue; Rutgers The State University of New Jersey, Mechanical and Aerospace Engineering Liang, Tongfen; Rutgers The State University of New Jersey, Mechanical and Aerospace Engineering Lopresti, Cora; Rutgers The State University of New Jersey, Mechanical and Aerospace Engineering Shukla, Smit; Rutgers The State University of New Jersey, Mechanical and Aerospace Engineering Akin, Meriem; Technische Universität Braunschweig, Institute of Microtechnology Weil, Brian; Rutgers The State University of New Jersey, Mechanical and Aerospace Engineering Hoque, Salman; Rutgers The State University of New Jersey, Mechanical and Aerospace Engineering Gruber, Emily; Rutgers The State University of New Jersey, Mechanical and Aerospace Engineering Mazzeo, Aaron; Rutgers The State University of New Jersey, Mechanical and Aerospace Engineering
Keyword:	Highly deformable robots < Robotics Field, soft locomotion < Robotics Field, soft manipulation < Robotics Field, continuum robot < Robotics Field
Manuscript Keywords (Search Terms):	paper-based actuators, soft robotics, origami robots, inflatable structures, finite element analysis

Note: The following files were submitted by the author for peer review, but cannot be converted to PDF. You must view these files (e.g. movies) online.

ZouVideo1.mp4
ZouVideo2.mp4
ZouVideo3.mp4
ZouVideo4.mp4

SCHOLARONE™
Manuscripts

Submitted to SoRo Soft Robotics

Paper-based Robotics with Stackable Pneumatic Actuators

Xiyue Zou[1], Tongfen Liang[1], Michael Yang[1], Cora LoPresti[1], Smit Shukla[1], Meriem Akin[2], Brian T. Weil[1], Salman Hoque[1], Emily Gruber[1], and Aaron D. Mazzeo[1*]

[1]Department of Mechanical and Aerospace Engineering, Rutgers University, 98 Brett Road, Piscataway, NJ 08854, USA

[2]Institute of Microtechnology, Braunschweiger University of Technology, Alte Salzdahlumer, 203 38124, Brunswick, Germany

For Peer Review

Submitted to SoRo Soft Robotics

Abstract

This work presents a unique approach to the design, fabrication, and characterization of paper-based robotic systems consisting of stackable pneumatic actuators. These paper-based actuators (PBAs) use materials with high elastic modulus-to-mass ratios, accordion-like structures, and direct coupling with pressure for extension and bending. The study contributes to our scientific and engineering understanding of foldable components under applied pressure through the construction of stretchable and flexible structures with intrinsically unstretchable and airtight materials. Experiments showed that a paper-based actuator possesses a power-to-weight ratio (PWR) greater than 80 W/kg, which is more than four times that of human muscle. This work also illustrates the stackability and functionality of paper-based actuators with two simple robotic systems: a parallel manipulator and a legged locomotor. The manipulator consists of an array of PBAs which can bend to a specific direction while inflating the corresponding actuator. In addition, the stacked actuators in the manipulator can rotate in opposite directions to compensate for relative rotation at the ends to work in parallel and manipulate the platform. The locomotor utilizes the rotation of PBAs to apply or release the friction between the feet and the ground. Furthermore, a numerical model of inflatable actuators included in this work predicts the qualitative mechanical performance of these actuators as a function of dimensional specifications and folding patterns. Overall, this work demonstrates how stacked paper-based materials can serve as actuators for robotic systems with light weight, foldability, and disposability. Future paper-based robots may be suitable for single use in contaminated or unstructured environments or for low-cost educational materials.

Keywords: paper-based actuators, soft robotics, origami robots, inflatable structures, finite element analysis

For Peer Review

Submitted to SoRo Soft Robotics

Introduction

Paper continues to receive attention as a material for electronics and robotics due to its low-cost, recyclability, and flexibility. Many state-of-the-art papertronic devices have included sensors[1–4], methods of energy storage[5–7], transistors[8–11], and electrochemical detectors.[12–14] In recent years, there has been an increasing amount of literature on origami/kirigami robots made of paper-like materials, which are advantageous due to a high elastic modulus-to-mass ratio and foldability. Origami and kirigami robots are capable of performing fundamental tasks of conventional rigid robots, such as walking, crawling, grasping, and manipulating.[15–23] Although paper-like materials are intrinsically unstretchable, these origami and kirigami robots, comparable to soft robots made of elastomers, are able to adapt to their surroundings or mimic the movement of living organisms, such as a worm and an octopus, by employing highly deformable structures.

Previous studies on elastomer-based actuators report multiple modes of actuation, including bending, extension, twisting, and rotation[24–36]; recent works have demonstrated that origami/kirigami actuators accomplished similar modes through employing highly deformable structures.[15–23,37,38] However, current origami and kirigami actuators may be limited in power and loading. The PWRs of many state-of-the-art pneumatic, elastomer-based actuators are several kW/kg at hundreds of kPa[39], while only two origami actuators with airtight layers in previous studies approached this level[37,38]. Martinez et al. presented several soft robotics actuators based on kirigami and origami structures consisting of paper-based skeletons and elastomeric coatings.[37] Their demonstrations showed that the payload-to-weight ratio of an elongating actuator with a mass of 8.3 g is 120. Li et al. developed origami-inspired artificial muscles made of PVC films at negative pressure.[38] The payload-to-weight ratio and power-to-weight ratio of these actuators with a massf of 2.6 g were 2 kW/kg and 384, respectively. These results suggest

For Peer Review

Submitted to SoRo Soft Robotics

that origami and kirigami actuators with an airtight structure or material may produce a higher power-to-weight ratio than human muscle to perform robotic tasks.

This study presents new and improved paper-based robotic systems designed with stackable paper-based actuators (PBAs), composed of sheets of paper, accordion-like structures, and direct coupling with pressure for extension and bending. Each PBA uses a common inflatable structure consisting of triangulated meshes, called Yoshimura patterns.[40] In 1955, Yoshimura discovered an inextensible displacement pattern that consisted of triangulated mesh patterns in a study on buckling of cylindrical shells under axial compression.[40] Over the past two decades, previous work has included the geometric description and kinematic analysis of origami structures with Yoshimura patterns (or Kresling patterns).[16,41–51] The extensive applications demonstrate the potential of these patterns to contribute to robotics[16,37,52], architecture[53,54], and deployable structures.[42,55] This work establishes how PBAs function in robotic systems with simple assembly. To illustrate the stackability of these foldable components, we give two simple examples: a parallel manipulator and a legged locomotor. These paper-based actuators may contribute to compliant, light-weight, and disposable robotic systems in the future.

For Peer Review

Materials and Methods

Principles of paper-based actuators

The stackable PBAs make use of four principles (see Figure 1). First, the folding patterns of these actuators are hexagonal Yoshimura patterns (see Figure S1 in Supplemental Materials). A folded actuator has several sections with repeated patterns and forms a tube with a hexagonal cross-section. Second, these PBAs elongate along their axial direction with pressurization. During the process of inflation, a PBA twists at both ends. The angle of rotation is 30° between

Submitted to SoRo Soft Robotics

both ends of each section with full extension. Third, a PBA with original Yoshimura patterns is a helix that rotates along its axial direction. To prevent its self-rotation, we reverse triangulated meshes at even-numbered sections. Forth, by tuning the stiffness of paper on the side, a PBA curves to its stiffer side. In this study, we employ a coating technique to reinforce regions of the actuators to tailor the curvature of their responses.

Like mechanical springs, PBAs can stack in series or parallel. PBAs connected in series stack end to end, so each PBA shares the same pneumatic channel that goes through the PBAs. By stacking actuators in series, we combine the motion of multiple PBAs, creating an actuator with new functionality. For example, if we connect one PBA with a stiffer left side and the other with a stiffer right side in series, they can curve to an S-shape with pressurization (see Figure 1B). PBAs connected in parallel share the same top and bottom ends, so their motions couple with each other. For PBAs connected in parallel, we can manipulate them by inflating different actuators. For example, two PBAs connected in parallel tilt right when inflating the left actuator; otherwise, they tilt left when inflating the right actuator (see Figure 1B).

Design and fabrication of paper-based actuators

These PBAs are simple to cut, fold, and seal. Figure S1 shows two types of Yoshimura patterns. The basal edge a and basal angle α are 24 mm and 30°, respectively. First, we used a commercial printer to print patterns on a piece of typical office paper with a grammage of 5 g to make the lines for cutting and folding the paper into a hexagonal tube. The cross-sectional area of the tube is 15 cm^2. Then, we used liquid glue (Elmer's Liquid School Glue) to seal the sides and attach two pieces of cardboard at both ends. Four sections in the middle were extensible, while the first and sixth section stayed attached to the top and bottom cardboard. We punched a hole in the bottom piece of cardboard and inserted a plastic tube fitting as an inlet for pressurized air. The

For Peer Review

Submitted to SoRo Soft Robotics

weight of a PBA with the tube fitting was 5 g and the original thickness is 9 mm in the compressed state. When folded patterns expanded fully, a PBA elongated 80 cm and rotated 120°. It is worth noting that these PBAs have no airtight layer, so air leaks from these actuators during inflation.

In this work, we used bendable PBAs as fingers of a gripper. We reduced the outer diameter of a PBA from 48 mm to 30 mm and increased the number of sections from six to twelve for making a thin and long actuator. Additionally, we used the folding patterns of non-rotatable PBAs to prevent sliding between grasped objects and the actuators. To tune the stiffness of paper, we brushed 0.6 mL of M-bond 200 adhesive on one side of an actuator. The liquid adhesive permeated paper and reinforced regions of the actuators after the adhesive cured. While curing, we sandwiched a group of bendable PBAs between two steel bars and compressed both ends of the tubes with the uncured adhesive to a length of 30 mm for setting their initial length. The cure time was 24 hours at room temperature.

Characterization of paper-based actuators

We characterized the mechanical performance of the PBAs experimentally. A rotatable PBA without reinforcement coating lifted 200 g of mass at 82.7 kPa (12 psi) in 0.5 seconds (see Figure 2A) for a power-to-weight ratio (PWR) of 80.7 W/kg which is more than four times that of human muscle (the PWR of human muscle is around 17.6 W/kg[56]). Not surprisingly, the PWR of these paper-based actuators without an airtight layer is lower than that of less leaky actuators reported in literature[37,38]. In this experiment, we tested two rotatable PBAs and two non-rotatable PBAs. We increased the pressure of pressurized air until the actuator lifted the payload to its highest position. As shown in Figure 2B, two actuators with the same folding patterns had similar behavior. It suggests that PBAs have a repeatable mechanical performance. Additionally,

For Peer Review

Submitted to SoRo Soft Robotics

non-rotatable PBAs required a higher pressure than rotatable PBAs for lifting the same payload to the highest position. The results suggest that the folding patterns of PBAs influence the mechanical performance of the actuators. For more details, see Supplemental Materials.

In addition, we characterized the bending and loading capability of bendable PBAs. As shown in Figure 3A, we fixed a bendable actuator on a test rig and used a camera to record the position of the actuator against a background of graph paper. We calculated the tilt angle of the top piece of cardboard and the elongation of the PBA in a horizontal direction, which are angle θ and the displacement of Point P in the horizontal direction d, respectively. When the pressure increased from 0 to 28 kPa, angle θ changed from 55° to 95°, and the displacement d was 12 mm. In the demonstration, the gripper consisted of four bendable PBAs. We characterized the loading capability of the gripper in Figure 3B (see Supplemental Materials for more details). In the demonstration, we used the gripper to grasp and lift small household objects in daily life, including plush toys, tapes, and snack food (see Video 1 in Supplemental Materials).

Modeling of paper-based actuators

To understand the mechanical performance of the foldable PBAs under applied pressure, we built a numerical model of the actuator in COMSOL. We applied a pressure, which increased linearly with time, to the inner surface of each triangular surface for simulating the pressurization. To simulate the unfolding process of the patterns, we swept the variable of time in a stationary study. As a result, the model simulated the process of inflation of a PBA from collapse to deployment (see Video 2 in Supplemental Materials). We described full details of the geometric formulation and modeling of a PBA in the Supplemental Materials (see Figure S2).

For Peer Review

Submitted to SoRo Soft Robotics

Figure 2C shows the deployment of rotatable Yoshimura patterns in the simulation. With the increase of pressure, the creases unfolded so that the shell elongated and rotated about the central axis of the tubular structure. To verify the model, we compared the numerical results to experimental data. In the experiment, we recorded the relationship between the elongation and rotation of a PBA for describing the unfolding process (see Figure S3 in Supplemental Materials for the experimental setup). Figure 2D shows that the deployment of the folding patterns in numerical solution matched well with that in experimental data, except an unrealistic peak around 6.5 cm. In the simulation, triangular surfaces in one side of the tube expands faster than those in other sides so the structure tilted slightly; however, in our experiments, triangular surfaces in all directions expanded evenly.

The model of the actuators has some limitations. First, the model did not consider the leakage of air. In the experiment, the pressure applied to the inner wall of an actuator is much less than the set pressure of the regulator, so the actuator in the experiment required a higher set pressure than the simulated pressure. Additionally, a higher set pressure drove leaky flow under hydrostatic pressure, which likely possessed a nonlinear relationship between the payload and the set pressure. Second, the model assumes that the creases and the triangular surfaces have the same material properties, so the mesh around creases has significant deformation when the actuator elongated. Though there is a difference between the model and an actual actuator, the comparison between simulation and experiment shows that the model can simulate the process of unfolding and predict the mechanical performance of the patterns. The model helps us to predict the outputs (such as the distribution of stress and the process of deployment) as a function of dimensional specifications, folding patterns, and nominal material properties.

Results

For Peer Review

Submitted to SoRo Soft Robotics

Design and demonstration of a parallel manipulator

The experimental results have demonstrated that the power-to-weight ratio of PBAs is higher than that of human muscle, so PBAs have the potential to grasp and transfer light-weight objects graspable by a single human hand. To show the potential applications of PBAs, we present a robotic arm consisting of a paper-based gripper (see Figure 3B) and a parallel manipulator (see Figure 4A).

We arranged three actuators into an equilateral triangle pattern and sandwiched them between two pieces of cardboard. We call the top and bottom pieces of cardboard as the "platform" and the "substrate", respectively (see Figure 4B). If the three actuators between the platform and substrate are three rotatable PBAs, the manipulator will lock because the twist of each actuator conflicts with the neighboring actuators. To avoid the lock of the manipulator, we connected two rotatable PBAs with mirrored symmetrical patterns in series. The upper PBA rotated clockwise, while the lower PBA rotated counter-clockwise. As a result, the twist of the two rotatable PBAs canceled out.

A LabVIEW interface with 8-channel solenoid valves allowed us to select the actuator we wanted to inflate. We used a pneumatic regulator to set the pressure of pressurized air and mounted the substrate of the manipulator on a test rig. Seven combinations of inflated actuators corresponded to seven directions of bending, which are $0°$, $\pm 60°$, $\pm 120°$, $180°$, and a vertical direction (see Figure 4A). When we tested the manipulator, we noticed that the deflation of the actuators had two problems. First, a part of the triangular meshes was unable to collapse so that the manipulator did not return to its original position. Second, even if all meshes collapsed, the deflation took a long time. The collapse of paper-based actuators is not a spontaneous process, so we used negative pressure to speed up the deflation of these actuators in the demonstration.

For Peer Review

Submitted to SoRo Soft Robotics

In the demonstration, we mounted a paper-based gripper to the platform of the manipulator (see Video 3 in Supplemental Materials). To speed up the collapse of folding patterns, we connected the networks of pressurized air to a vacuum pump with a pressure of − 88.3 kPa and kept the pump turning on during the whole demonstration. We increased the pressure of pressurized air to 103 kPa to neutralize the suction of the negative pressure. As shown in Figure 4C, the manipulator bent to a Ping-Pong ball at its left side, grasped the ball, bent to its right side, and dropped the ball in a container. This demonstration shows that a manipulator consisting of PBAs can realize a pick-and-place function.

Design and demonstration of a legged locomotor

The second application is a legged locomotor (See Figure 5). We utilize the elongation and twist of rotatable PBAs to apply or release the friction between the feet of the locomotor and the ground, so it walks with a stick-slip motion. As shown in Figure 5A, the locomotor consists of two actuators in parallel, called “Left Actuator” and “Right Actuator”. Each actuator consists of two PBAs with mirrored symmetrical patterns in series (see Figure 5A). To create a contact interface, we mounted two T-shaped paper-folded feet on both ends of Left/Right Actuator. To prevent the locomotor from moving backward, we changed the coefficient of friction at the front and rear half of the interface. We attached a rubber film made of Mold Star 30 (Smooth-On Inc.) to the bottom of each foot and used a piece of tape to cover the front half of the film.

In the demonstration, we connected Left/Right Actuator to a network of tubing in which the tubing of compressed air of each actuator connected with that of a vacuum pump (see Figure 5B). In this setup, the suction of negative pressure speeded up the deflation of Left/Right Actuator for a longer walking distance at each step. Additionally, we clamped the tubing on a support stand to decrease the friction between the tubing and the ground (see Figure S5). The

For Peer Review

Submitted to SoRo Soft Robotics

demonstration includes three cases. In the first case, we used a support stand to clamp pipes and used negative pressure to deflate the actuators. In the second case, we clamped pipes but did not use negative pressure. In the third case, we let the locomotor drag the tubing on the ground and did not use negative pressure. The latter two cases show the influence of the suction of negative pressure and the friction of tethers on the locomotor. As shown in Video 4 in Supplemental Materials, the walker walked 11 cm in 20 seconds in the first case (see Figure 5B). To track the position of the walker, we attached a piece of tape with red dye to the top of the framework and extracted the position of the red dye via image processing. Figure 5C shows the relationship between time and the position of the locomotor in each case. The average velocity was 5.2 mm/s, 2.9 mm/s, and 1.7 mm/s in the first, second, and third case, respectively. In the first case, the average velocity of the locomotor was close to 7 mm/s in the first 10 seconds. With the increase of the walking distance, the locomotor dragged the tubing on the ground, so the velocity decreased with the increase of friction between the tubing and the ground.

In the demonstration, we show that a robotic system consisted of PBAs in series and parallel can implement complex motions, although a single PBA can only implement simple motions, such as elongation and rotation.

Discussion

This work provides a unique method to design robots made of thin-sheet materials, such as origami robots. We designed stackable actuators and stacked these actuators to implement a series of specific and complex motions. Although there have been other origami-inspired pneumatic actuators[22,37,38,42], this study is the first, to our knowledge, of paper-based robotic systems which consist of stackable, pneumatic actuators. Although the property of PBAs limited the performance of the robots in this paper, researchers may enhance the performance of the

For Peer Review

Submitted to SoRo Soft Robotics

robotic systems by improving the design, material, and fabrication of the stackable actuator in the future.

To understand the mechanical performance of PBAs, we experimentally characterized the actuators and numerically simulated their unfolding process. The experimental results suggest that the power-to-weight ratio of a PBA is more than four times that of human muscle. To predict the mechanical performance of PBAs as a function of the folding patterns, we create a numerical model to simulate the unfolding process of inflatable structures, and the results match well with the experimental data. The model has the potential to guide the design of origami actuators made of paper or other thin-sheet materials in the future. Two robotic systems illustrated the extensive applications of these stackable actuators. These paper-based robots with high deformable structures showed similar properties of elastomer-based robots, even though paper is not stretchable.[57] For examples, the underactuated gripper adapts to the shape of its targeted objects; the manipulator exhibits tentacle-like behavior, which has theoretically finite degree of freedom; the locomotor shows similarity to earthworms which extend/contract their body when moving forward. This study may have an impact on the structural design and choice of materials of compliant robotics.

Furthermore, these robots are low-cost, recyclable, and deployable. In the future, paper-based manipulators have the potential to transfer and manipulate small and fragile objects, such as medical/biomedical samples in healthcare facilities. The primary material of the robot is paper so that users can recycle or burn them for sterilization after use. Additionally, paper-based locomotors have the potential to inspect unstructured quarters and transport tether-like payloads, such as signal wires and flexible tubing for beverages and liquid food. A robot with folded components may also be capable of navigating channels, cavities, or chambers with narrow

For Peer Review

Submitted to SoRo Soft Robotics

cross-sectional regions. The low-cost and accessible nature of paper may facilitate the use of paper-based robotics for educational demonstrations and learning in the classroom.

Acknowledgements

The authors acknowledge support from National Science Foundation Award Nos. 1610933 and 1653584. X.Z. and T.L. acknowledge fellowships from the China Scholarship Council. M.A. acknowledges support from the IP@Leibniz program.

Author's contributions

X.Z., T.L., M.A., and A.D.M. designed the research; X.Z., M.Y., C.L., S.S., B.W., S.H., and A.D.M. performed the research; X.Z., T.L., and A.D.M. analyzed the data; and X.Z., M.A., E.G., and A.D.M. wrote the paper.

Author disclosure statements

The authors declare no conflict of interest.

For Peer Review

Submitted to SoRo Soft Robotics

Reference

1. Koehly R. Fabrication of Sustainable Resistive-Based Paper Touch Sensors: Application to Music Technology. Ph.D., McGill University (Canada): Canada, 2011.
2. Liu X, Mwangi M, Li X, O'Brien M, Whitesides GM. Paper-Based Piezoresistive MEMS Sensors. Lab Chip. 2011;11(13):2189–2196.
3. Zou X, Chen C, Liang T, Xie J, Gillette-Henao E-N, Oh J, Tumalle J, Mazzeo AD. Paper-Based Resistive Networks for Scalable Skin-Like Sensing. Advanced Electronic Materials. 2018;4(8):1800131.
4. Akin M, Pratt A, Blackburn J, Dietzel A. Paper-Based Magneto-Resistive Sensor: Modeling, Fabrication, Characterization, and Application. Sensors. 2018;18(12):4392.
5. Ferreira I, Brás B, Correia N, Barquinha P, Fortunato E, Martins R. Self-Rechargeable Paper Thin-Film Batteries: Performance and Applications. J. Display Technol., JDT. 2010;6(8):332–335.
6. Lee H, Choi S. A Micro-Sized Bio-Solar Cell for Self-Sustaining Power Generation. Lab Chip. 2014;15(2):391–398.
7. Li S, Huang D, Zhang B, Xu X, Wang M, Yang G, Shen Y. Flexible Supercapacitors Based on Bacterial Cellulose Paper Electrodes. Adv. Energy Mater. 2014;4(10):n/a-n/a.
8. Fortunato E, Correia N, Barquinha P, Costa C, Pereira L, Gonçalves G, Martins R. Paper Field Effect Transistor. In; 2009; Vol. 7217, pp. 72170K-72170K – 11.
9. Berggren M, Nilsson D, Robinson ND. Organic Materials for Printed Electronics. Nature Materials. 2007;6(1):3–5.
10. Zocco AT, You H, Hagen JA, Steckl AJ. Pentacene Organic Thin-Film Transistors on Flexible Paper and Glass Substrates. Nanotechnology. 2014;25(9):094005.
11. Martins R, Barquinha P, Pereira L, Correia N, Gonçalves G, Ferreira I, Fortunato E. Write-Erase and Read Paper Memory Transistor. Applied Physics Letters. 2008;93203501.
12. Dungchai W, Chailapakul O, Henry CS. Electrochemical Detection for Paper-Based Microfluidics. Anal. Chem. 2009;81(14):5821–5826.
13. Liu H, Crooks RM. Paper-Based Electrochemical Sensing Platform with Integral Battery and Electrochromic Read-Out. Anal. Chem. 2012;84(5):2528–2532.
14. Li X, Liu X. A Microfluidic Paper-Based Origami Nanobiosensor for Label-Free, Ultrasensitive Immunoassays. Adv. Healthcare Mater. 2016;5(11):1326–1335.
15. Miyashita S, Guitron S, Ludersdorfer M, Sung CR, Rus D. An Untethered Miniature Origami Robot That Self-Folds, Walks, Swims, and Degrades. In; IEEE, 2015; pp. 1490–1496.
16. Pagano A, Yan T, Chien B, Wissa A, Tawfick S. A Crawling Robot Driven by Multi-Stable Origami. Smart Materials and Structures. 2017;26(9):094007.
17. Rafsanjani A, Zhang Y, Liu B, Rubinstein SM, Bertoldi K. Kirigami Skins Make a Simple Soft Actuator Crawl. Science Robotics. 2018;3(15):eaar7555.
18. Shigemune H, Maeda S, Hara Y, Hosoya N, Hashimoto S. Origami Robot: A Self-Folding Paper Robot With an Electrothermal Actuator Created by Printing. IEEE/ASME Transactions on Mechatronics. 2016;21(6):2746–2754.
19. Felton S, Tolley M, Demaine E, Rus D, Wood R. A Method for Building Self-Folding Machines. Science. 2014;345(6197):644–646.
20. Niiyama R, Rus D, Kim S. Pouch Motors: Printable/Inflatable Soft Actuators for Robotics. In; IEEE, 2014; pp. 6332–6337.

For Peer Review

Submitted to SoRo Soft Robotics

21. Chen AS, Zhu H, Li Y, Hu L, Bergbreiter S. A Paper-Based Electrostatic Zipper Actuator for Printable Robots. In; IEEE, 2014; pp. 5038–5043.
22. Du X, Wu H, Qi J, Jeong SY, Ni F. Paper-Based Pneumatic Locomotive Robot with Sticky Actuator. MATEC Web of Conferences. 2016;4203014.
23. Kim Y, Yuk H, Zhao R, Chester SA, Zhao X. Printing Ferromagnetic Domains for Untethered Fast-Transforming Soft Materials. Nature. 2018;558(7709):274–279.
24. Ilievski F, Mazzeo AD, Shepherd RF, Chen X, Whitesides GM. Soft Robotics for Chemists. Angewandte Chemie. 2011;123(8):1930–1935.
25. Pelrine R, Kornbluh R, Joseph J, Heydt R, Pei Q, Chiba S. High-Field Deformation of Elastomeric Dielectrics for Actuators. Materials Science and Engineering: C. 2000;11(2):89–100.
26. Shepherd RF, Ilievski F, Choi W, Morin SA, Stokes AA, Mazzeo AD, Chen X, Wang M, Whitesides GM. Multigait Soft Robot. Proceedings of the National Academy of Sciences. 2011;108(51):20400–20403.
27. Gong X, Yang K, Xie J, Wang Y, Kulkarni P, Hobbs AS, Mazzeo AD. Rotary Actuators Based on Pneumatically Driven Elastomeric Structures. Adv. Mater. 2016;287533–7538.
28. Suzumori K. Elastic Materials Producing Compliant Robots. Robotics and Autonomous Systems. 1996;18(1):135–140.
29. Morin SA, Shepherd RF, Kwok SW, Stokes AA, Nemiroski A, Whitesides GM. Camouflage and Display for Soft Machines. Science. 2012;337(6096):828–832.
30. Ferraresi C, Franco W, Bertetto AM. Straight Fibres Pneumatic Muscle : An Actuator with High Traction Force. In; 1999; pp. 787–798.
31. Tolley MT, Shepherd RF, Mosadegh B, Galloway KC, Wehner M, Karpelson M, Wood RJ, Whitesides GM. A Resilient, Untethered Soft Robot. Soft Robotics. 2014;1(3):213–223.
32. Marchese AD, Katzschmann RK, Rus D. A Recipe for Soft Fluidic Elastomer Robots. Soft Robotics. 2015;2(1):7–25.
33. Cianchetti M, Ranzani T, Gerboni G, Nanayakkara T, Althoefer K, Dasgupta P, Menciassi A. Soft Robotics Technologies to Address Shortcomings in Today's Minimally Invasive Surgery: The STIFF-FLOP Approach. Soft Robotics. 2014;1(2):122–131.
34. Galloway KC, Becker KP, Phillips B, Kirby J, Licht S, Tchernov D, Wood RJ, Gruber DF. Soft Robotic Grippers for Biological Sampling on Deep Reefs. Soft Robotics. 2016;3(1):23–33.
35. Manti M, Hassan T, Passetti G, D'Elia N, Laschi C, Cianchetti M. A Bioinspired Soft Robotic Gripper for Adaptable and Effective Grasping. Soft Robotics. 2015;2(3):107–116.
36. Robertson MA, Sadeghi H, Florez JM, Paik J. Soft Pneumatic Actuator Fascicles for High Force and Reliability. Soft Robotics. 2017;4(1):23–32.
37. Martinez RV, Fish CR, Chen X, Whitesides GM. Elastomeric Origami: Programmable Paper-Elastomer Composites as Pneumatic Actuators. Adv. Funct. Mater. 2012;22(7):1376–1384.
38. Li S, Vogt DM, Rus D, Wood RJ. Fluid-Driven Origami-Inspired Artificial Muscles. PNAS. 2017;201713450.
39. Daerden F, Lefeber D. Pneumatic Artificial Muscles: Actuators for Robotics and Automation. European Journal of Mechanical and Environmental Engineering. 2002;47(1).
40. Yoshimaru Yoshimura. On the Mechanism of Buckling of a Circular Cylindrical Shell under Axial Compression. 1955.

For Peer Review

Submitted to SoRo Soft Robotics

41. Evans TA, Lang RJ, Magleby SP, Howell LL. Rigidly Foldable Origami Gadgets and Tessellations. Royal Society Open Science. 2015;2(9):150067.
42. R.J.P. BARKER, S.D. GUEST. Inflatable Triangulated Cylinders. In; Springer, Dordrecht, 2000; pp. 17–26.
43. Guest SD, Pellegrino S. The Folding of Triangulated Cylinders, Part II: The Folding Process. Journal of Applied Mechanics. 1994;61(4):778.
44. Guest SD, Pellegrino S. The Folding of Triangulated Cylinders, Part III: Experiments. Journal of Applied Mechanics. 1996;63(1):77.
45. Guest SD, Pellegrino S. The Folding of Triangulated Cylinders, Part I: Geometric Considerations. Journal of Applied Mechanics. 1994;61(4):773.
46. Ishida S, Nojima T, Hagiwara I. Regular Folding Pattern for Deployable Nonaxisymmetric Tubes [1]. Journal of Mechanical Design. 2015;137(9):091402.
47. Zhai Z, Wang Y, Jiang H. Origami-Inspired, on-Demand Deployable and Collapsible Mechanical Metamaterials with Tunable Stiffness. Proceedings of the National Academy of Sciences. 2018;115(9):2032–2037.
48. Hunt GW, Ario I. Twist Buckling and the Foldable Cylinder: An Exercise in Origami. International Journal of Non-Linear Mechanics. 2005;40(6):833–843.
49. Jianguo C, Xiaowei D, Yuting Z, Jian F, Ya Z. Folding Behavior of a Foldable Prismatic Mast With Kresling Origami Pattern. Journal of Mechanisms and Robotics. 2016;8(3):031004.
50. Jianguo C, Xiaowei D, Ya Z, Jian F, Yongming T. Bistable Behavior of the Cylindrical Origami Structure With Kresling Pattern. Journal of Mechanical Design. 2015;137(6):061406.
51. Jared Thomas Bruton. Packing Sheet Materials Into Cylinders and Prisms Using Origami-Based Approaches. Masters Thesis, Brigham Young University: Utah, USA, 2016.
52. Onal CD, Wood RJ, Rus D. Towards Printable Robotics: Origami-Inspired Planar Fabrication of Three-Dimensional Mechanisms. In; IEEE, 2011; pp. 4608–4613.
53. Stavrić M, Siđanin P, Tepavčevic′ B. *Architectural Scale Models in the Digital Age: Design, Representation and Manufacturing*; Springer: Wien, 2013.
54. N. Sugiura, Y. Nakamura, H. Tagawa, T. Uno, S. Okazaki. Design and Fabrication of Origami Dome. In *Arch-Cultural Interations through the Silk Road, 4th International Conference*; Mukogawa Women's Univ., Nishinomiya, Japan, 2016.
55. Wilson L, Pellegrino S, Danner R. Origami Sunshield Concepts for Space Telescopes. In; American Institute of Aeronautics and Astronautics, 2013.
56. Ryder JW, Buxton RE, Goetchius E, Scott-Pandorf M, Hackney KJ, Fiedler J, Ploutz-Snyder RJ, Bloomberg JJ, Ploutz-Snyder LL. Influence of Muscle Strength to Weight Ratio on Functional Task Performance. European Journal of Applied Physiology. 2013;113(4):911–921.
57. Chen A, Yin R, Cao L, Yuan C, Ding HK, Zhang WJ. Soft Robotics: Definition and Research Issues. In *2017 24th International Conference on Mechatronics and Machine Vision in Practice (M2VIP)*; IEEE: Auckland, 2017; pp. 366–370.

For Peer Review

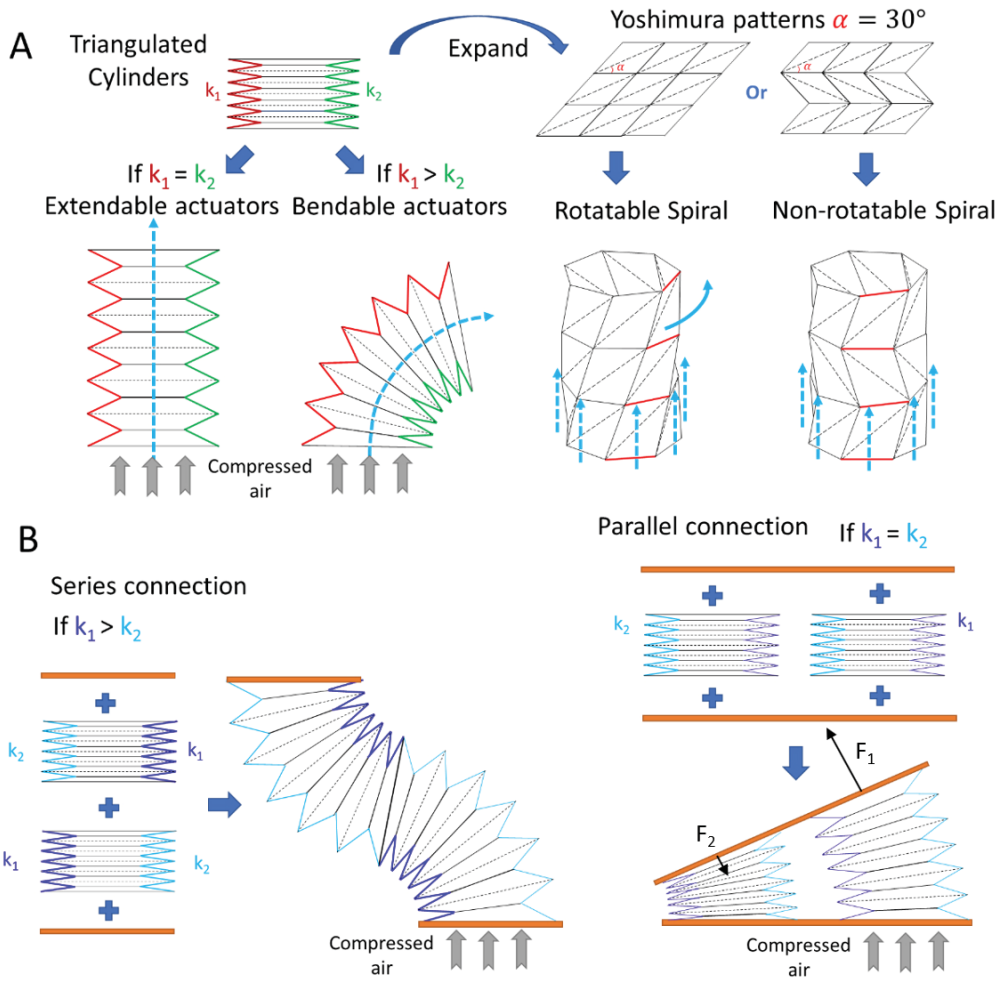

Figure 1.

Figure 1. Schematics of paper-based actuators. (A) The design of PBAs and their tunable stiffness. A PBA can curve to one side by tuning the stiffness of paper on the side. A PBA with original Yoshimura patterns rotates with deployment. By reversing triangulated meshes at specified sections, a PBA can elongate without rotation. (B) PBAs in series and parallel. An example of PBAs in series is an S-shaped actuator which consists of a PBA with a stiffer right side and a PBA with a stiffer left side. An example of PBAs in parallel is a parallel manipulator with two PBAs.

238x245mm (120 x 120 DPI)

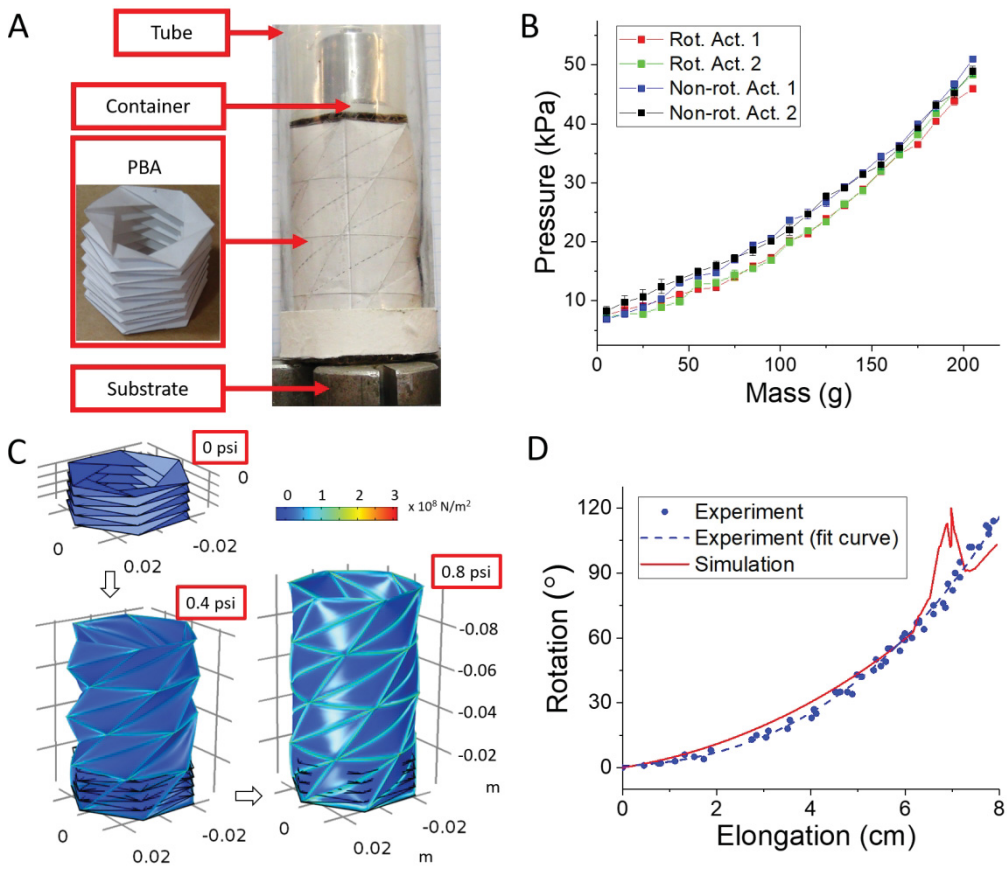

Figure 2.

Figure 2. The experiment and simulation of the deployment of PBAs. (A) The experimental setup of the characterization of PBAs. A tube supported the actuator for avoiding buckling. The figure shows a PBA lifted 200 g of mass at 44.8 kPa. (B) The relationship between payload and pressure. The pressure in the y-axis is the minimum pressure for lifting the payload to the highest position. The test repeated three times. (C) The process of the deployment of a rotatable PBA. The color scale shows the first principal strain on the shell. (D) The comparison of the elongation and rotation of a rotatable PBA between experiment and simulation.

374x343mm (120 x 120 DPI)

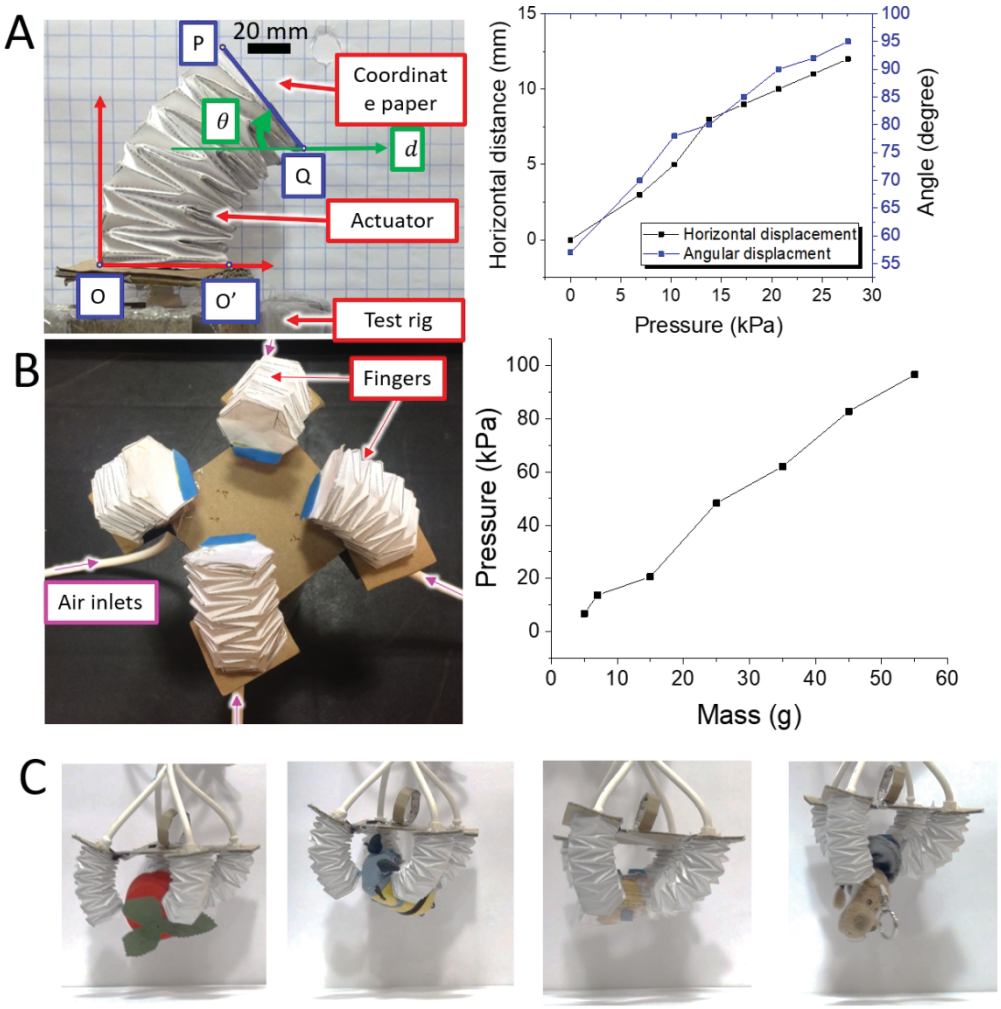

Figure 3.

Figure 3. The experiment and demonstration of bendable PBAs and a paper gripper. (A) The characterization of a bendable PBA. Angle θ is the angular displacement of the top piece of cardboard. Vector d is the displacement of the actuator in a horizontal direction. (B) The design and characterization of the gripper. The chart on the right side shows the relationship between the mass of payload and the minimum pressure for lifting the payload. (C) The demonstration of the gripper. The figure shows that the gripper lifted plush toys and snack food.

262x276mm (120 x 120 DPI)

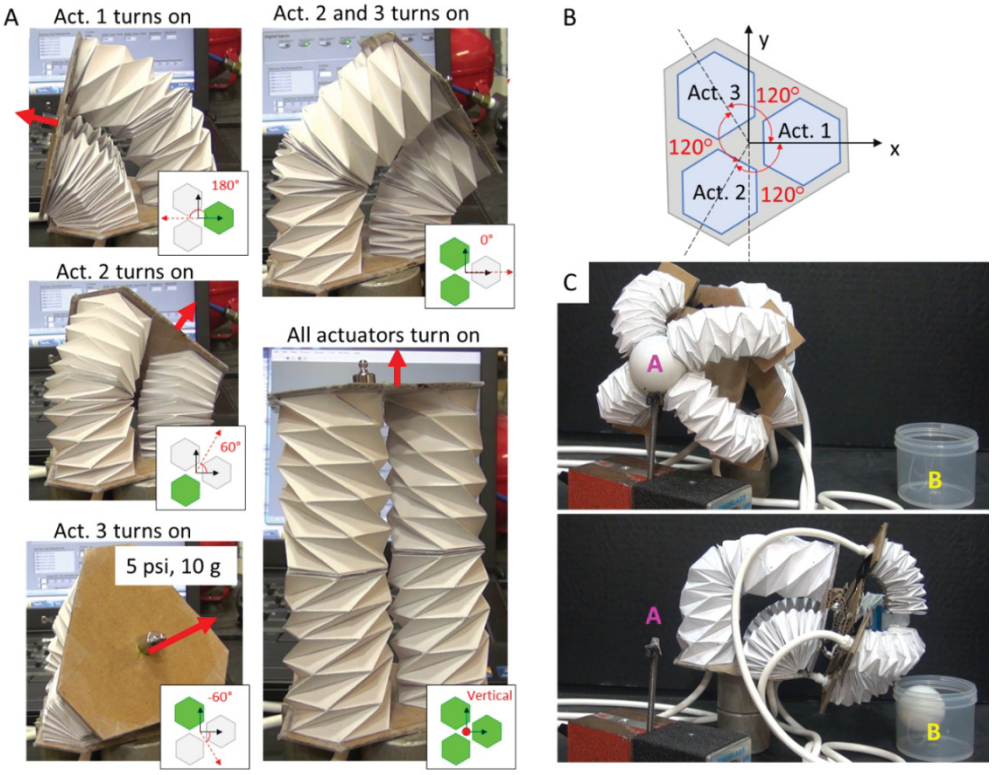

Figure 4.

Figure 4. The demonstration of a manipulator consisted of PBAs. (A) The direction of bending of a parallel manipulator. The green hexagon is the inflated actuator. The red arrow is the direction of bending. (B) Schematics of a manipulator. We placed three actuators in a triangle pattern. The figure shows the definition of the coordinate of the manipulator. (C) The demonstration of a manipulator. The manipulator transferred a ball from Point A to B.

266x218mm (120 x 120 DPI)

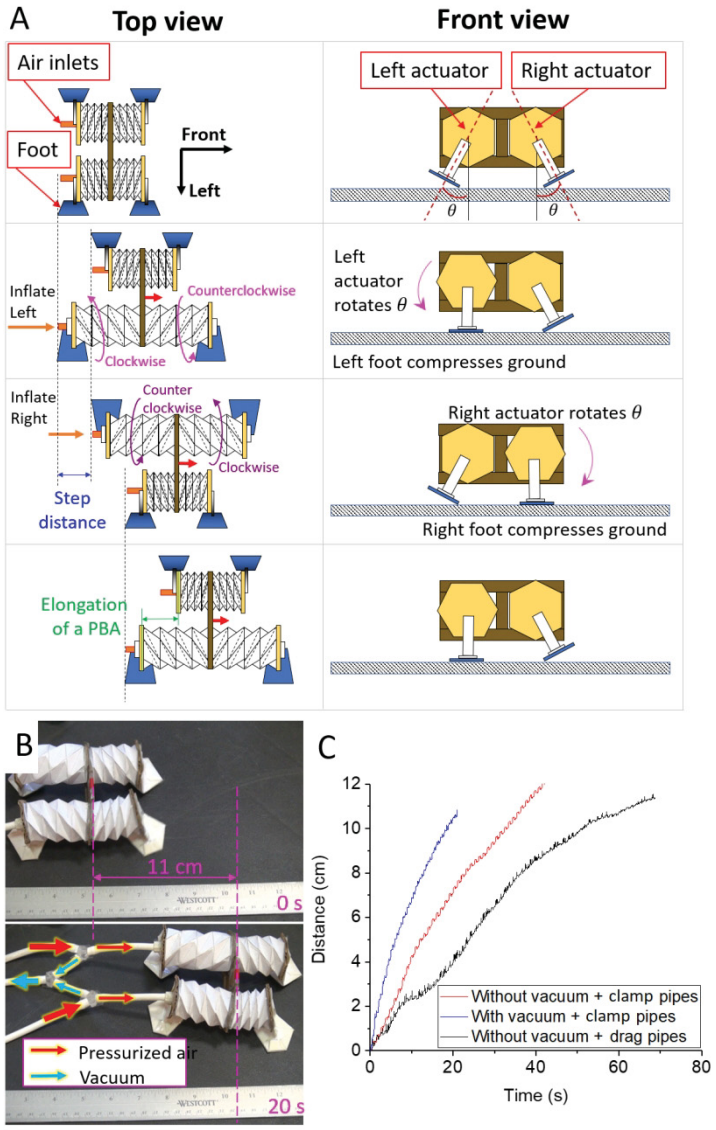

Figure 5.

Figure 5. The design and demonstration of a legged locomotor. (A) The diagram of a locomotor. We marked the direction of rotation of each PBA as arrows. Assume that the locomotor does not slide back, the walking distance at each step is equal to the elongation of each PBA. (B) The demonstration and photographs of the locomotor. The red arrow is the direction of pressurized air. The blue arrow is the direction of vacuum. (C) The relationship between time and walking distance. In the third case, the locomotor had significant backsliding at each step because of the friction of its tubing. In the second case, though the locomotor has backsliding, the locomotor had a longer walking distance at each step because of the application of a vacuum.

278x420mm (120 x 120 DPI)

Submitted to SoRo Soft Robotics

Paper-based Robotics with Stackable Pneumatic Actuators

Supplemental Materials

Xiyue Zou[1], Tongfen Liang[1], Michael Yang[1], Cora LoPresti[1], Smit Shukla[1], Meriem Akin[2], Brian T. Weil[1] Salman Hoque[1], Emily Gruber[1], and Aaron D. Mazzeo[1*]

[1]Department of Mechanical and Aerospace Engineering, Rutgers University, 98 Brett Road, Piscataway, NJ 08854, USA

[2]Institute of Microtechnology, Braunschweiger University of Technology, Alte Salzdahlumer, 203 38124, Brunswick, Germany

For Peer Review

Submitted to SoRo Soft Robotics

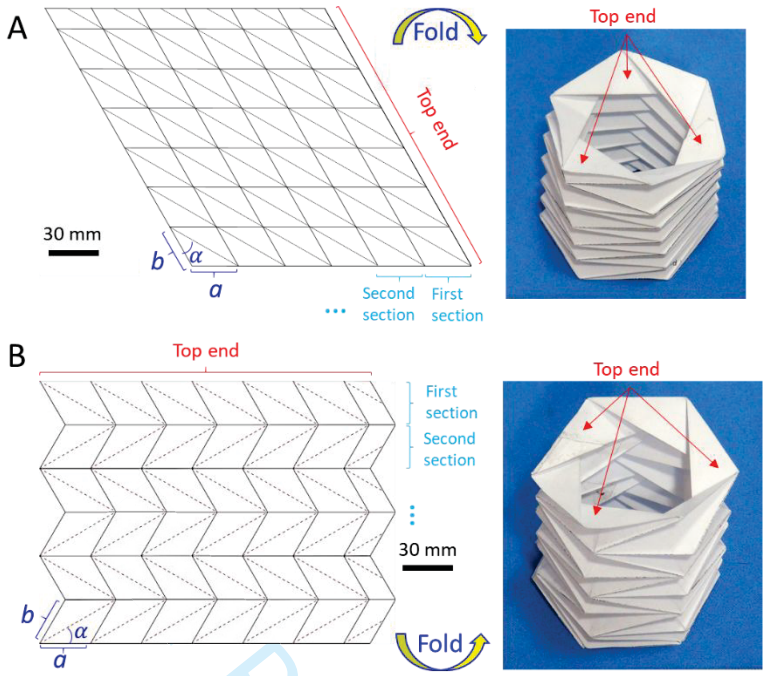

Figure S1. The folding patterns of hexagonal Yoshimura patterns. The solid lines mean mountain fold, and the dashes mean valley fold. The folding patterns include six sections; each section consists of six rhombuses with an angle of 60°. For one rhombus, each edge requires a mountain fold, and the longer diagonal requires a valley fold. The longer diagonal of each rhombus divides the rhombus into two triangles; this triangle is the basic unit of the folding patterns. In each unit, the basal angle α is 30° and the basal length, *a* and *b*, is the length of the two short edges of the triangle. (A) Rotatable actuator and its folding patterns. (B) Non-rotatable actuator and its folding patterns. Its folding patterns reverse at each section.

Peer Review

Submitted to SoRo Soft Robotics

The setup and method of experimental characterization of PBAs

In the experiment, we used a portable electric air compressor to provide compressed air. To protect valves and adjust the pressure, we used a pneumatic regulator to limit the pressure of compressed air below 103 kPa (15 psi). We mounted a PBA on a test rig and attached weights to its top. Without any extra support, a single actuator buckled if the mass of weights was above 30 g. To prevent the buckling of an actuator, we needed an experimental setup that can support the applied weights but avoid direct contact with the tested actuator. We put weights into a cylindrical container with a 60 mm diameter, placed the container on the top of the PBA without any attachment, and inserted the actuator into a glass tube (see Figure 2A). The outer diameter of the container is larger than that of the actuator so that the tube can support the container from its sides, instead of contact with the actuator.

At the beginning of the experiment, we put the empty container (5 g) to the top of the tested actuator and pressurized it with 0.68 kPa (0.1 psi). If the actuator approached its maximum length ($\geq$ 10.5 mm), we recorded the pressure, applied 10 g weights to the container, and repeated the test; if not, we increased 0.68 kPa pressure and repeated the test. We tested two rotatable and two non-rotatable actuators, which have the same basal length and basal angle.

The modeling and simulation of a PBA

To model a foldable actuator, we calculated the coordinate of each vertex in three-dimensional space. Each floor consists of 12 triangulated surfaces and 12 vertices (see SI Figure 2), in which the six vertices in the top end rotates around z axis. According to geometrical relationship, all vertices are on a cylindrical surface with a radius R, the distance from the center to each vertex. Thus, the coordinates of six points on the substrate, which is in plane $z = 0$ are knowns. Let us

For Peer Review

Submitted to SoRo Soft Robotics

assume that the coordinates of two points are knowns on triangle $P_1P_2P_3$, which is $P_1(P_{1x}, P_{1y}, P_{1z})$ and $P_2(P_{2x}, P_{2y}, P_{2z})$. To fine the coordinate of $P_3(P_{3x}, P_{3y}, P_{3z})$, we use three equations as shown in Eq. 1 to Eq. 3.

$$P_{3x}{}^2 + P_{3y}{}^2 = R^2 \quad \text{(Eq. 1)}$$

$$(P_{3x} - P_{2x})^2 + (P_{3y} - P_{2y})^2 = R^2 \quad \text{(Eq. 2)}$$

$$n_x \cdot P_{3x} + n_y \cdot P_{3y} + n_z \cdot P_{3z} + 1 = 0 \quad \text{(Eq. 3)}$$

In the equations, Eq. 1 means that point P_3 is on the cylindrical surface; Eq. 2 means that the distance between point P_2 and point P_3 is R; Eq. 3 means that point P_3 is in the plane of triangular mesh $P_1P_2P_3$, and (n_x, n_y, n_z) is the normal vector of the plane. To find the normal vector of the plane, we need three more equations as shown in Eq. 4 to Eq. 6.

$$n_x \cdot P_{1x} + n_y \cdot P_{1y} + n_z \cdot P_{1z} + 1 = 0 \quad \text{(Eq. 4)}$$

$$n_x \cdot P_{2x} + n_y \cdot P_{2y} + n_z \cdot P_{2z} + 1 = 0 \quad \text{(Eq. 5)}$$

$$\cos\left(\frac{\pi}{180}\theta\right) = \frac{n_z}{\sqrt{n_x{}^2 + n_y{}^2 + n_z{}^2}} \quad \text{(Eq. 6)}$$

Eq. 4 and Eq. 5 illustrate that point P_1 and P_2 are on the plane; Eq. 6 means that the angle between z axis and the plane is θ, which is a variable. We use the solve system of nonlinear equations in MATLAB R2018 to solve above equations for finding the coordinate of point P_3. We can use the same method to find each point in the actuator. Figure S2 shows a 3D plot of the first floor of an actuator with $\theta = 15°$.

After we get the coordinate of all points, we can model each triangular mesh in COMSOL. The collapsed model we used is the model when $\theta = 5°$. The thickness of the shell is 0.05 mm, which is the thickness of paper in the experiment. We set the material property of all boundaries to the

For Peer Review

Submitted to SoRo Soft Robotics

property of paper, in which elastic modulus, Poisson's ratio, and density are 2.5 GPa, 0.25, and 800 kg/m^3. To simulate the procedure of inflation, we use stationary study to solve the model with a swept variable, which is the pressure applied to each inner surface. In the setting section of stationary, it is necessary to check the option "Include geometric nonlinearity" for calculating the deformation of structure in the large scale. Additionally, the factor "Maximum number of iterations" should be a large number around 500 for convergence. As a result, we can get a series of solutions till the actuator approaches its maximum length.

The numerical model can simulate the procedure of inflation of a PBA, but there is a difference between experiment and simulation. In the simulation, we didn't consider pressure loss in pipes and air leakage in the actuator, so the pressure applied to an actual actuator is less than the reading pressure at the pneumatic regulator. For an instance, an actuator in experiments fully elongates at 7.1 kPa, which is higher than the pressure 5.5 kPa in simulation.

Although the difference between experiment and simulation is non-neglectable, the simulation helps us to understand the mechanical properties of these foldable/stretchable components. For an example, Figure 2 shows a comparison between non-rotatable and rotatable actuators at different loads. The relationship between applied pressurization and elongation has a slight difference before and after reversing patterns at each floor, so it indicates that the modification of structure changes the mechanical properties of PBAs. In Figure S4, the results in simulation match well with these in experiments: two actuators require about the same pressure to reach the maximum length when no pressure applies, while non-rotatable actuator requires a lower pressure than rotatable one to reach the same length when 50 g loads applies.

For Peer Review

Submitted to SoRo Soft Robotics

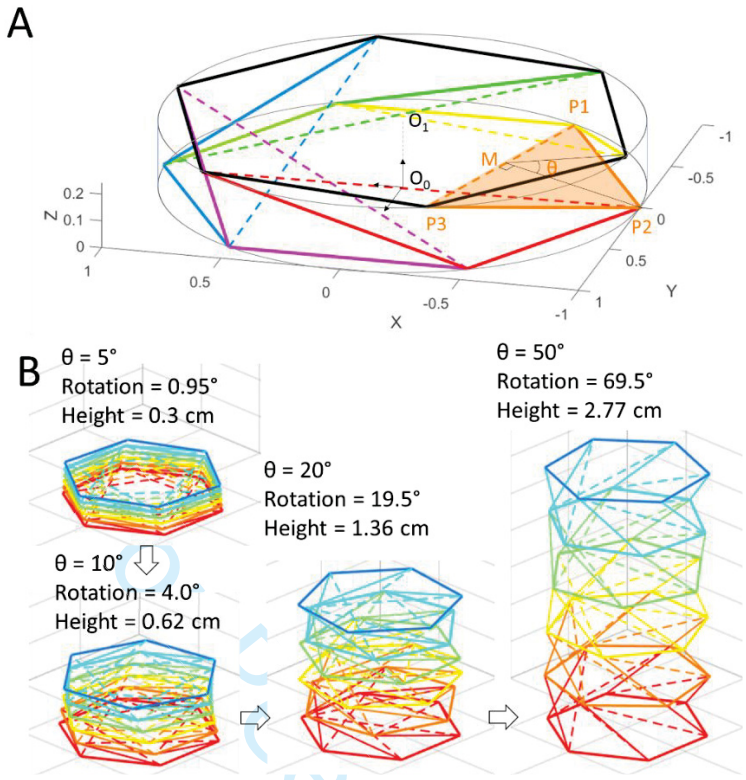

Figure S2. The geometrical formulation of one floor of Yoshimura pattern. The length of edge is 1 cm. (a) Modeling of the patterns. The straight lines and axis are plotted in MATLAB, and the variable θ is 15°. (B) The rotation and height of an actuator in different angel θ.

Peer Review

Submitted to SoRo Soft Robotics

Design and characterization of a underactuated gripper

To make a gripper, we mounted four bendable PBAs at four corners of a piece of cardboard. We turned the reinforced regions of PBAs to the center of the cardboard and connected the tube fitting of each finger to the inlet of pressurized air. When pressurized air flowed in the inlet, four fingers simultaneously extended and curved to the center of the gripper. To characterize the load capacity of the gripper, we put payload into a cylindrical container with a diameter of 60 mm and increased the pressure of pressurized air until it picked up the container. As shown in Figure 3B, the pressure increased linearly with the mass of payload, and the gripper grasped a mass of 50 g at 96.5 kPa.

Design and experimental setup of a legged locomotor

The locomotor consists of two actuators in parallel. We call the two actuators at the left and right sides as “Left Actuator” and “Right Actuator”, respectively. Each actuator consists of two PBAs with mirror symmetry in series (see Figure 5A). The basal length of the folding patterns is 15 mm. The actuators of the locomotor are similar to that of the manipulator but differ in the linkage of PBAs in parallel. We used a piece of cardboard to link the two actuators in the location of their junction, rather than the top and bottom ends. To create a contact interface between PBAs and the ground, we mounted two T-shaped paper-folded feet on both ends of Left/Right Actuators. When an actuator elongated, its two feet contacted the ground; when the actuator collapsed, its two feet left the ground because of the twist of rotatable PBAs. For a collapsed PBA, the angle between the ground and its foot is 30°. To prevent the locomotor from moving backward, we changed the coefficient of friction at the front and rear half of the contact

For Peer Review

Submitted to SoRo Soft Robotics

interface. We attached a film made of Mold Star 30 (Smooth-On Inc.) to the bottom of each foot and used a piece of tape to cover the front half of the film.

We programmed the control system to actuate the locomotor. As shown in Figure 5A, the first step was to inflate the Right Actuator and deflate the Left Actuator; the second step was to inflate the Left Actuator and deflate the Right Actuator. When we deflated an actuator, both feet of the actuator left the ground. When we inflated an actuator, both feet contacted the ground, and the front foot slipped to the forward direction because of the coefficient of friction of the front half foot is lower than that of the rear half foot. The interval of each step was 0.5 seconds. By repeating the two steps, the locomotor kept moving forward.

For Peer Review

Submitted to SoRo Soft Robotics

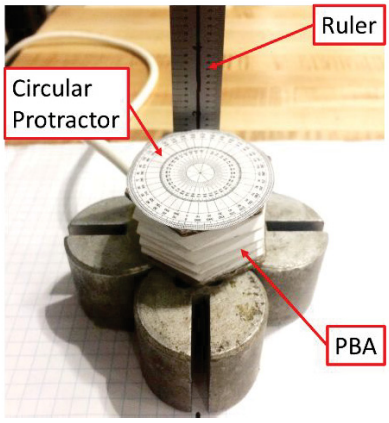

Figure S3. The experimental setup for measuring the rotation and elongation of a PBA. We used a ruler to measure the elongation of the actuator and used a circular protractor to measure the rotation of its top surface. We increased the pressure of compressed air and recorded the rotation and elongation of the actuator in each step. We repeated the test five times.

For Peer Review

Submitted to SoRo Soft Robotics

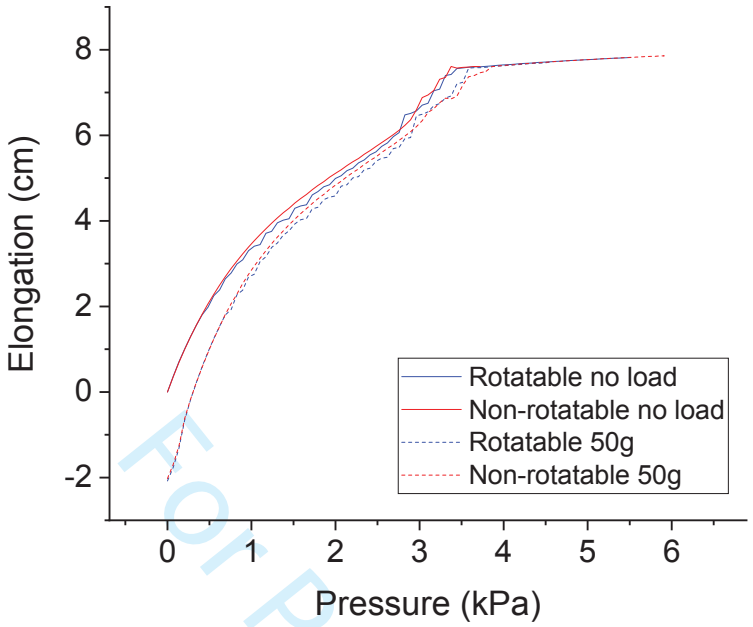

Figure S4. Numerical resolutions of rotatable/non-rotatable paper-based actuators with/without loading. The origin of y-axis is the initial position of the top surface of the actuator when no loads applies. The variable α is 15°, so the actuator has an initial compression when applied loads to the top of the actuator.

For Peer Review

Submitted to SoRo Soft Robotics

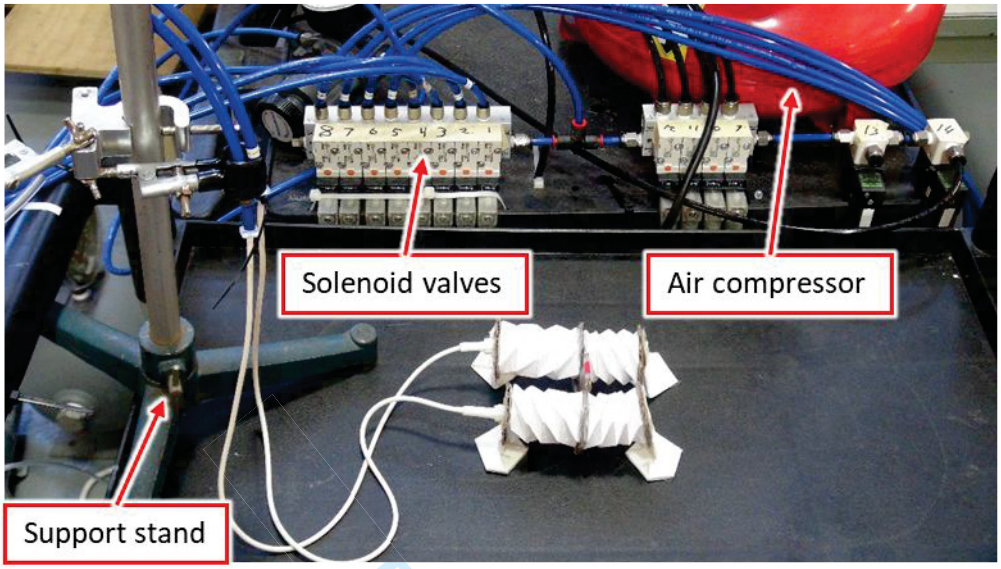

Figure S5. The experimental setup of a legged locomotor with hanging pipes.

Peer Review